



Cite this: *Chem. Commun.*, 2016, 52, 974

Received 26th August 2015,
Accepted 13th November 2015

DOI: 10.1039/c5cc07171b

www.rsc.org/chemcomm

Design of amine-functionalized metal–organic frameworks for CO₂ separation: the more amine, the better?†

Zhiwei Qiao,^a Nanyi Wang,^b Jianwen Jiang^c and Jian Zhou^{*a}

A total of 41 825 metal–organic frameworks (MOFs) were computationally screened toward the design of amine-functionalized MOFs for CO₂ separation. Both the optimal species and number of amine functional groups were examined for eight MOFs with good performance in terms of CO₂ uptake and selectivity. It was revealed that more amine functional groups grafted on the MOFs do not lead to a better CO₂ separation capability, and the concept of saturation degree of functional groups was proposed. The ethylenediamine-functionalized MOF-74 membrane was predicted to possess high CO₂ permeation separation capability, which was confirmed by the parallel experimental test of gas permeation.

Metal–organic frameworks (MOFs) have received tremendous interest in the past few decades due to their large potential for H₂ storage,¹ CO₂ capture,² catalysis,³ gas separation and purification,⁴ liquid separation⁵ and drug delivery.⁶ However, the performance of many synthesized MOFs cannot satisfy industrial demands. Therefore, their functionalized counterparts have attracted considerable attention because they are more effective compared with the original ones, such as their higher separation efficiency,⁷ gas storage,⁸ catalytic performance⁹ and luminescence capability.¹⁰

H₂ and CH₄ are considered as environmentally friendly energy carriers and have received much attention. Nevertheless, the presence of CO₂ in them remarkably decreases their heat values. Moreover, in a moist environment, CO₂ can react with water to produce carbonic acid, leading to corrosive effects

not only on the equipment but also on the pipes during transportation.¹¹ Consequently, CO₂ separation from H₂ or CH₄ is crucial in the processing of clean fuels. Toward this end, the functionalization of MOFs by amine functional groups has been recognized as an effective technique to improve the adsorption and separation of acidic CO₂.¹² In the literature, a larger number of amine-functionalized MOFs have been synthesized and tested.¹³ Vaidhyanathan *et al.*¹⁴ reported the crystallographic resolution of amine-functionalized MOFs and their analysis showed that the low-pressure binding and large uptake of CO₂ were influenced by three factors, *i.e.*, strongly interacting amine functional groups, suitable pore size and the cooperative binding of CO₂ molecules. Ahnfeldt *et al.*¹⁵ synthesized four amine-functionalized MOFs including CAU-1-NH₂, CAU-1-NHCH₃, CAU-1-NH₂(OH) and CAU-1-NHCOCH₃, and examined the effects of time and temperature.

While a wide variety of MOFs can be modified for CO₂ separation, it remains elusive which specific MOFs are suitable to be functionalized, which functional groups have the best improvement and what is the optimal number of functional groups. In most experimental efforts, many MOFs were modified by trial-and-error, resulting in a slight chance of successful synthesis and actual enhancement in performance. It is thus of great significance to unravel how functionalized MOFs can be rationally designed from a computational approach and then efficiently synthesized. Recently, large-scale computational screening has been conducted for gas storage and separation in MOFs.¹⁶ From 138 000 hypothetical MOFs, Snurr and coworkers identified over 300 MOFs with a predicted CH₄ storage capacity better than any known materials;¹⁷ they further proposed correlations between structural/chemical characteristics and adsorption criteria for CO₂ separation.¹⁸ Similarly, Woo and coworkers reported the large-scale quantitative structure–property relationship for CH₄ storage.¹⁹

In this study, we focus on the design of optimal species and number of amine functional groups to functionalize MOFs toward high CO₂ separation. The MOFs selected for functionalization were first computationally screened from a large database.

^a School of Chemistry and Chemical Engineering, South China University of Technology, Guangdong Provincial Key Lab for Green Chemical Product Technology and State Key Lab of Pulp and Paper Engineering, Guangzhou 510640, China. E-mail: jianzhou@scut.edu.cn

^b Institute of Physical Chemistry and Electrochemistry, Leibniz University of Hannover, Callinstrasse 22, 30167 Hannover, Germany

^c Department of Chemical and Biomolecular Engineering, National University of Singapore, 117576, Singapore

† Electronic supplementary information (ESI) available: Simulation and experimental details, SEM images, XRD patterns, CO₂ isotherms and selectivities. See DOI: 10.1039/c5cc07171b

Then, the effects of different amine functional groups on CO₂ adsorption and selectivity in functionalized MOFs were systematically examined. Finally, the designed MOF with a superior performance was experimentally synthesized and tested.

41 825 MOFs were computationally screened in this work and then selected for amine functionalization. Among them, 29 have been experimentally synthesized as collected in Table S1 (ESI[†]), including the well-known subfamilies and newly synthesized ones. The rest were hypothetical un-functionalized MOFs selected from the database developed by Snurr and coworkers.¹⁷ We expect the large-scale screening of the wide variety of MOFs would give ideal candidates for the design of amine-functionalized materials. CO₂/CH₄ mixtures were considered at their practical states in industry (Table S2, ESI[†]). In addition, the adsorption in Al-MIL-53 and Cr-MIL-53 was only calculated at high pressures because of their breathing effect.²⁰ Based on the adsorption loadings and selectivities shown in Fig. 2, eight MOFs including M-MOF-74 (M = Mg, Ni, Co, Zn), Al-MIL-53, Cr-MIL-53, UiO-66 and UiO-67 were selected since they exhibit remarkable adsorption capacities and separation factors, as well as they are experimentally available. These eight MOFs were further examined by amine functionalization to improve CO₂ separation capability.

Furthermore, four different amine functional groups (–NH₂, –NHCH₂CH₂NH₂, –NHCOH, –NHCOCH₃) (see Fig. S2, ESI[†]) were used to modify the eight selected MOFs. We also intend to identify their optimal number of amine functional groups. For Al-MIL-53, Cr-MIL-53, UiO-66 and UiO-67, their active functional sites are in the BDC ligand, thus three numbers (1, 2, 4) of different groups per unit cell were chosen to modify their original frameworks. For M-MOF-74, because the active functional sites are in the metal ligand,²¹ five (1, 3, 6, 9, 18) amine group numbers per unit cell were used, as shown in Fig. 1.

Altogether there are 48 functionalized Al-MIL-53, Cr-MIL-53, UiO-66 and UiO-67 (four MOFs, four amine functional groups and three amine group numbers, 4 × 4 × 3 = 48) with similar active functional sites. In Fig. S4a and S6a (ESI[†]), it can be seen that Al-MIL-53 and Cr-MIL-53 modified by the –NHCOH group show the best separation factors among the 48 functionalized MOFs, while their adsorption loadings are in the intermediate level. The separation factors of –NHCOH functionalized Al-MIL-53, Cr-MIL-53, UiO-66 and UiO-67 are much higher than those modified by the other amine functional groups, although the

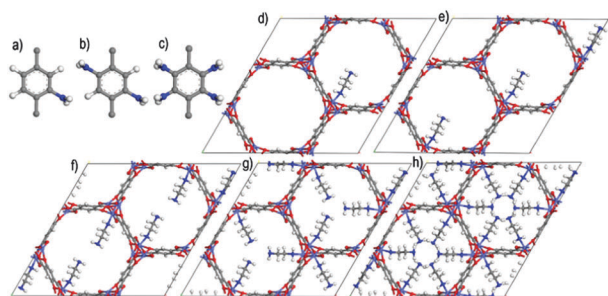


Fig. 1 1,4-Benzenedicarboxylate (BDC) structures with (a) 1, (b) 2 and (c) 4 amines and unit cell structures of M-MOF-74 with (d) 1, (e) 3, (f) 6, (g) 9 and (h) 18 ethylene diamines per unit cell.

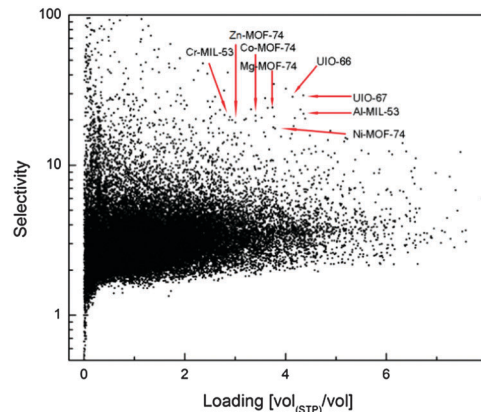


Fig. 2 Comparison of adsorption selectivities and total loadings of 41 825 MOFs for CO₂/CH₄ separation at 5 bar and 298 K.

loadings are similar. Therefore, we infer that the –NHCOH modification of the BDC ligand promotes CO₂ separation, especially for (NHCOH)_n–Al-MIL-53. Furthermore, Fig. S4c, d and S27a–34a (ESI[†]) show the loading drops; however, the separation factor rises with the increase in the number of amine functional groups. Thus, the more amine functional groups in the four MOFs, the stronger interactions and charge effects exist with CO₂ molecules leading to higher loadings. From the contours of electrostatic potentials (ESPs) in Fig. S5 (ESI[†]), the difference of charge effects between Al-MIL-53 and (NHCOH)₄–Al-MIL-53 is clearly observed. The –NHCOH group has a large effect on the two sides of the organic linker. The higher ESP absolute values of (NHCOH)₄–Al-MIL-53 reflect a larger electrostatic potential compared with that of Al-MIL-53, which enhances the CO₂ separation selectivity. Finally, the simulation reveals that when more amine functional groups are grafted into the four MOFs, the MOFs have a better CO₂ separation capability; the –NHCOH group is most suitable for the modification of Al-MIL-53, Cr-MIL-53, UiO-66 and UiO-67.

There exist 80 kinds of amine-functionalized M-MOF-74 (four different metal ligands, four amine functional groups and five different numbers of amine functional groups, 4 × 4 × 5 = 80). Firstly, it is interesting to find that the amine-functionalized Co-MOF-74 has the most superior separation factor for CO₂/CH₄, whereas the highest loading is in Mg-MOF-74, shown in Fig. S7 (ESI[†]). This is because the interactions between the metal ligands and CO₂ molecules are drastically weakened upon amine functionalization. Most CO₂ molecules adsorbed in the unmodified Co-MOF-74 are distributed near the metal ligands, so the high-separation area is near the metal ligand, as shown in Fig. S9a (ESI[†]). Nevertheless, the high separation area in amine-functionalized Co-MOF-74 is at around the amine functional groups, especially at the center of three amine functional groups. Secondly, it can be clearly to seen from Fig. 3a–c that the performance order for the separation factor of different amine functional groups is –NHCH₂CH₂NH₂ > –NH₂ or –NHCOH > and –NHCOCH₃. One of reasons is that –NHCH₂CH₂NH₂ has two active amine functional groups, which possess more specific interactions with CO₂ molecules. Another reason is that the

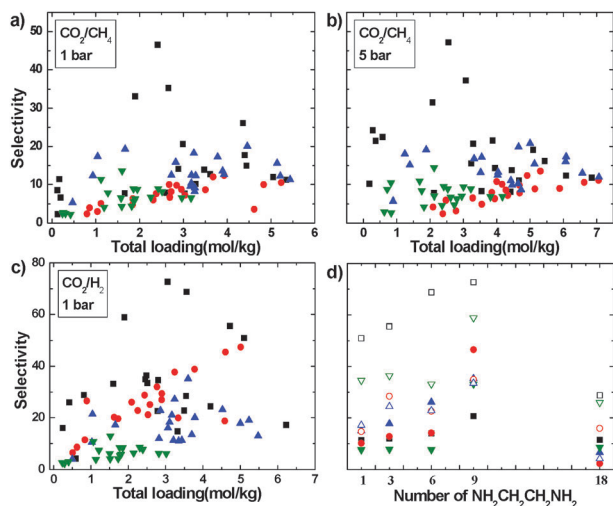


Fig. 3 Comparison of total loadings and adsorption selectivities of different amine functional group modified M-MOF-74 at 298 K, (a) 1 bar for CO_2/CH_4 , (b) 5 bar for CO_2/CH_4 and (c) 1 bar for CO_2/H_2 . Black \blacksquare : $\text{NHCH}_2\text{CH}_2\text{NH}_2$; red \bullet : NH_2 ; blue \blacktriangle : NHCOH ; and green \blacktriangledown : NHCOCH_3 . (d) Selectivity numbers of $\text{NHCH}_2\text{CH}_2\text{NH}_2$ group relations. Solid \blacksquare : 1 bar for CO_2/CH_4 ; hollow \square : 1 bar for CO_2/H_2 ; black \blacksquare : Mg-MOF-74; red \bullet : Co-MOF-74; blue \blacktriangle : Ni-MOF-74; green \blacktriangledown : Zn-MOF-74.

larger pore size of M-MOF-74 (see Table S1, ESI[†]) allows functionalization by the amine group with a longer chain (e.g. $-\text{NHCH}_2\text{CH}_2\text{NH}_2$). Finally, Fig. 3d shows that the separation factor reaches the maximum when the number of amine functional groups per unit cell is 9. For Al-MIL-53, Cr-MIL-53, UiO-66 and UiO-67, we have revealed above that MOFs with more amine functional groups have a higher separation factor. However, the influence of the amine group number for M-MOF-74 is different: when the number exceeds 9 and reaches 18 per unit cell, both the separation factor and adsorption loading drop tremendously. Thus, the saturation degree of amine functional groups depends on the type of MOFs, and it is 9 per unit cell for M-MOF-74. Upon comparing the separation factor distribution of $(\text{NH}_2\text{CH}_2\text{CH}_2\text{NH})_9\text{-Co-MOF-74}$, shown in Fig. S9b (ESI[†]), the center of the triangle-like $-\text{NHCH}_2\text{CH}_2\text{NH}_2$ groups is the region with high separation selectivity due to a strong potential overlap. In contrast, MOFs grafted with other numbers of amine functional groups cannot form triangle-like adsorption regions. Therefore, the triangle-like structure is the primary reason for the high selectivity of M-MOF-74 modified with 9 amine functional groups per unit cell.

We simulated simultaneously the gas diffusivities in 20 $(\text{NH}_2\text{CH}_2\text{CH}_2\text{NH})_n\text{-M-MOF-74}$, which have the most remarkable separation efficiency. Both the adsorption loadings and diffusivities were employed to calculate the gas permeability and permeation selectivity. The simulation results were compared with the experimental results, shown in Fig. 4 and Fig. S10 (ESI[†]). It could be observed in Fig. 4 that with the increase in amine functional groups, the gas permeability keeps a decreasing trend; whereas the permeation selectivity increases firstly and then decreases; and when the modification group number is 9 per unit cell, the overall performance reaches the peak.

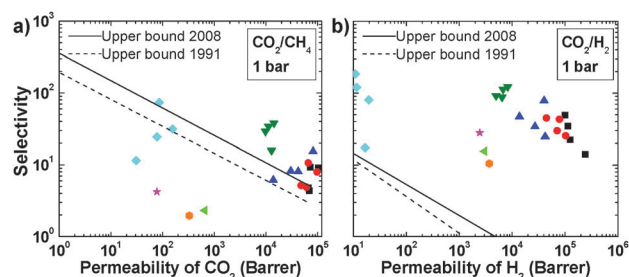


Fig. 4 Comparison of permeability and permeation selectivity of different $(\text{NH}_2\text{CH}_2\text{CH}_2\text{NH})_n\text{-M-MOF-74}$ at 298 K, (a) 1 bar for CO_2/CH_4 and (b) 1 bar for CO_2/H_2 . Black \blacksquare : 1; red \bullet : 3; blue \blacktriangle : 6; green \blacktriangledown : 9; cyan \blacklozenge : 18; turquoise \blacktriangleleft : simulated unmodified Mg-MOF-74; orange \bullet : experimental unmodified Mg-MOF-74 membrane; and pink \star : experimental $\text{NH}_2\text{CH}_2\text{CH}_2\text{NH-Mg-MOF-74}$ membrane.

Thus, the saturation degree of amine functional groups is also suitable to predict the separation capability of MOF membranes. Upon comparing the data modified by 1 $-\text{NHCH}_2\text{CH}_2\text{NH}_2$ group (black) with that by 9 $-\text{NHCH}_2\text{CH}_2\text{NH}_2$ groups (green), we could find that the former has the highest permeability, but, considering the tradeoff between permeability and permeation selectivity, the latter is thought to have a higher performance. All of the M-MOF-74 modified by 9 amine functional groups per unit cell exceeded the upper bound line, as by Robeson.²² Moreover, the simulation data of the unmodified Mg-MOF-74 (turquoise) for two mixtures were in very good agreement with the experimental results (orange). The experimental result of amine-modified MOFs for H_2/CO_2 (pink) was in the range of simulation results with different functional groups. The separation performance of the computer-design-guided amine-modified MOF is significantly improved when compared with that of unmodified MOF.

Because of the predicted high loading and separation capability for H_2/CO_2 , the ethylene-diamine-functionalized Mg-MOF-74 membrane was fabricated. As shown by the SEM image in Fig. S11 (ESI[†]), the membrane is dense and largely defect-free. Furthermore, the XRD patterns of the Mg-MOF-74 powder (Fig. S12, ESI[†]) are in good agreement with the reported work²³ and the FT-IR spectra (Fig. S13, ESI[†]) prove that the Mg-MOF-74 membrane was grafted by the $-\text{NHCH}_2\text{CH}_2\text{NH}_2$ group. The permeation selectivities of H_2/CO_2 and CH_4/CO_2 were measured. After the amination of the open Mg sites, the separation performance of the Mg-MOF-74 membrane was remarkably enhanced; the H_2/CO_2 selectivity is increased from 12.2 to 29 at room temperature. The CH_4/CO_2 selectivity of the ethylene-diamine-functionalized Mg-MOF-74 is two times that of the original one. It verifies that the computationally designed amine-functionalized MOF can improve the CO_2 separation efficiency.

In this study, a large-scale computational screening was conducted on 41 825 MOFs and then eight MOFs were selected for further functionalization to improve CO_2 separation. The suitable amine functional groups and the optimal number of functional groups for each MOF were examined toward the design of a preferable amine functionalization route. The simulation results show that $-\text{NHCOH}$ for the BDC ligand of Al-MIL-53, Cr-MIL-53, UiO-66 and UiO-67 is the most suitable group and

the MOFs with more amine functional groups have a higher separation factor. In M-MOF-74; however, the amine group with a long chain such as $\text{-NHCH}_2\text{CH}_2\text{NH}_2$ can enhance the CO_2 separation efficiency more remarkably than other groups. It was revealed that the saturation degree of amine functional groups for M-MOF-74 is 9 per unit cell and the triangle-like structure in M-MOF-74 modified by 9 amine functional groups per unit cell is favorable for CO_2 separation. Finally, an ethylenediamine-functionalized Mg-MOF-74 membrane was synthesized. It exhibits a superior performance when compared with its unmodified counterpart. The preferable amine-modified routes, the concept of saturation degree of functional groups, the high CO_2 separation characteristics, along with the triangle locations of three amine functional groups in the pore of M-MOF-74 could provide insightful guidance to develop new functionalized MOFs for gas separation.

This work was supported by National Key Basic Research Program of China (No. 2013CB733500), the National Natural Science Foundation of China (No. 21376089 and 91334202), China Postdoctoral Science Foundation (No. 2014M560663), Guangdong Science Foundation (No. 2014A030312007 and 2014A030310206), the Fundamental Research Funds for the Central Universities (SCUT-2014ZB0012, 2015ZP033), the State Key Lab of Pulp and Paper Engineering Program (No. 201444), and the National University of Singapore for CENGas (Center of Excellence for Natural Gas) (R261-508-001-646/733). The computational resources were provided by SCUTGrid at the South China University of Technology and the National University of Singapore. The authors gratefully thank Prof. Randall Q. Snurr for providing the database of hMOFs, Prof. Tom K. Woo for providing the MEPO-QEq code, and Prof. Jürgen Caro for the guidance of experiments.

Notes and references

- 1 D. Fairen-Jimenez, Y. J. Colón, O. Farha, Y. S. Bae, J. T. Hupp and R. Q. Snurr, *Chem. Commun.*, 2012, **48**, 10496–10498.
- 2 Y.-S. Bae and R. Q. Snurr, *Angew. Chem., Int. Ed.*, 2011, **50**, 11586–11596.
- 3 U. Mueller, M. Schubert, F. Teich, H. Puetter, K. Schierle-Arndt and J. Pastre, *J. Mater. Chem.*, 2006, **16**, 626–636.
- 4 (a) T. R. C. Van Assche and J. F. M. Denayer, *Chem. Eng. Sci.*, 2013, **95**, 65–72; (b) L. H. Lu, S. S. Wang, E. A. Mueller, W. Cao, Y. D. Zhu, X. H. Lu and G. Jackson, *Fluid Phase Equilib.*, 2014, **362**, 227–234; (c) Z. J. Bian, X. Zhu, T. Jin, J. Gao, J. Hu and H. L. Liu, *Microporous Mesoporous Mater.*, 2014, **200**, 159–164.
- 5 (a) B. Liu, O. Shekhhah, H. K. Arslan, J. Liu, C. Wöll and R. A. Fischer, *Angew. Chem., Int. Ed.*, 2012, **51**, 807–810; (b) Z. Qiao, A. Torres-Knoop, D. Fairen-Jimenez, D. Dubbeldam, J. Zhou and R. Q. Snurr, *AIChE J.*, 2014, **60**, 2324–2334.
- 6 A. C. McKinlay, R. E. Morris, P. Horcajada, G. Férey, R. Gref, P. Couvreur and C. Serre, *Angew. Chem., Int. Ed.*, 2010, **49**, 6260–6266.
- 7 (a) N. Planas, A. L. Dzubak, R. Poloni, L.-C. Lin, A. McManus, T. M. McDonald, J. B. Neaton, J. R. Long, B. Smit and L. Gagliardi, *J. Am. Chem. Soc.*, 2013, **135**, 7402–7405; (b) Z. Qiao, J. Zhou and X. H. Lu, *Fluid Phase Equilib.*, 2014, **362**, 342–348.
- 8 (a) S. Najafi Nobar and S. Farooq, *Chem. Eng. Sci.*, 2012, **84**, 801–813; (b) Y. He, X. Zhu, Y. Li, C. Peng, J. Hu and H. L. Liu, *Microporous Mesoporous Mater.*, 2015, **214**, 181–187.
- 9 P. V. Dau and S. M. Cohen, *Chem. Commun.*, 2013, **49**, 6128–6130.
- 10 A. M. Marti, N. Nijem, Y. J. Chabal and K. J. Balkus Jr, *Microporous Mesoporous Mater.*, 2013, **174**, 100–107.
- 11 S. Li, J. L. Falconer and R. D. Noble, *J. Membr. Sci.*, 2004, **241**, 121–135.
- 12 (a) Z. Wang, M. Fang, Y. Pan, S. Yan and Z. Luo, *Chem. Eng. Sci.*, 2013, **93**, 238–249; (b) P. Bröder, K. G. Lauritsen, T. Mejdell and H. F. Svendsen, *Chem. Eng. Sci.*, 2012, **75**, 28–37.
- 13 (a) B. Arstad, H. Fjellvåg, K. O. Kongshaug, O. Swang and R. Blom, *Adsorption*, 2008, **14**, 755–762; (b) S. Couck, J. F. M. Denayer, G. V. Baron, T. Rémy, J. Gascon and F. Kapteijn, *J. Am. Chem. Soc.*, 2009, **131**, 6326–6327; (c) A. M. Fracaroli, H. Furukawa, M. Suzuki, M. Dodd, S. Okajima, F. Gándara, J. A. Reimer and O. M. Yaghi, *J. Am. Chem. Soc.*, 2014, **136**, 8863–8866.
- 14 R. Vaidhyanathan, S. S. Iremonger, G. K. H. Shimizu, P. G. Boyd, S. Alavi and T. K. Woo, *Science*, 2010, **330**, 650–653.
- 15 T. Ahnfeldt, D. Gunzelmann, J. Wack, J. Senker and N. Stock, *CrystEngComm*, 2012, **14**, 4126–4136.
- 16 (a) Y. J. Colon and R. Q. Snurr, *Chem. Soc. Rev.*, 2014, **43**, 5735–5749; (b) M. C. Bernini, D. Fairen-Jimenez, M. Pasinetti, A. J. Ramirez-Pastor and R. Q. Snurr, *J. Mater. Chem. B*, 2014, **2**, 766–774; (c) A. Torres-Knoop, R. Krishna and D. Dubbeldam, *Angew. Chem., Int. Ed.*, 2014, **53**, 7774–7778.
- 17 C. E. Wilmer, M. Leaf, C. Y. Lee, O. K. Farha, B. G. Hauser, J. T. Hupp and R. Q. Snurr, *Nat. Chem.*, 2012, **4**, 83–89.
- 18 C. E. Wilmer, O. K. Farha, Y. S. Bae, J. T. Hupp and R. Q. Snurr, *Energy Environ. Sci.*, 2012, **5**, 9849–9856.
- 19 M. Fernandez, T. K. Woo, C. E. Wilmer and R. Q. Snurr, *J. Phys. Chem. C*, 2013, **117**, 7681–7689.
- 20 N. A. Ramsahye, G. Maurin, S. Bourrelly, P. L. Llewellyn, T. Loiseau, C. Serre and G. Férey, *Chem. Commun.*, 2007, 3261–3263.
- 21 S. Choi, T. Watanabe, T.-H. Bae, D. S. Sholl and C. W. Jones, *J. Phys. Chem. Lett.*, 2012, **3**, 1136–1141.
- 22 L. M. Robeson, *J. Membr. Sci.*, 2008, **320**, 390–400.
- 23 Z. Bao, L. Yu, Q. Ren, X. Lu and S. Deng, *J. Colloid Interface Sci.*, 2011, **353**, 549–556.